






## ORIGINAL ARTICLE

Drug Allergy, Insect Sting Allergy, and Anaphylaxis

# Nanoarchitectures for efficient IgE cross-linking on effector cells to study amoxicillin allergy

Amene Tesfaye<sup>1,2</sup>  | Alba Rodríguez-Nogales<sup>1,2</sup> | Sara Benedé<sup>3</sup> |  
 Tahía D. Fernández<sup>2,4</sup>  | Juan L. Paris<sup>1,2</sup> | María J. Rodríguez<sup>1,2</sup> |  
 Isabel M. Jiménez-Sánchez<sup>1,2</sup> | Gador Bogas<sup>2,5</sup> | Cristobalina Mayorga<sup>1,2,5</sup>  |  
 María J. Torres<sup>1,2,5,6</sup>  | María I. Montañez<sup>1,2</sup> 

<sup>1</sup>Andalusian Centre for Nanomedicine and Biotechnology-BIONAND, Málaga, Spain

<sup>2</sup>Allergy Research Group, Instituto de Investigación Biomédica de Málaga-IBIMA, Málaga, Spain

<sup>3</sup>Instituto de Investigación en Ciencias de la Alimentación (CIAL, CSIC-UAM), Madrid, Spain

<sup>4</sup>Departamento de Biología Celular Genética y Fisiología, Facultad de Ciencias, Universidad de Málaga, Málaga, Spain

<sup>5</sup>Allergy Unit, Hospital Regional Universitario de Málaga, Málaga, Spain

<sup>6</sup>Departamento de Medicina, Facultad de Medicina, Universidad de Málaga, Málaga, Spain

## Correspondence

María I. Montañez, Andalusian Center for Nanomedicine and Biotechnology-BIONAND, Parque Tecnológico de Andalucía, 29590 Málaga, Spain.  
 Email: maribel.montanez@ibima.eu

## Funding information

European Union's H2020 research and innovation programme under the Marie Skłodowska-Curie, Grant/Award Number: 713721; Andalusian Regional Ministry Health, Grant/Award Number: RC-0004-2021, PI-0699-2011 and PI-0179-2014; Institute of Health "Carlos III", Grant/Award Number: PI12/02529, PI15/01206, PI18/00095, CP15/00103,

## Abstract

**Background:** Amoxicillin (AX) is nowadays the  $\beta$ -lactam that more frequently induces immediate allergic reactions. Nevertheless, diagnosis of AX allergy is occasionally challenging due to risky *in vivo* tests and non-optimal sensitivity of *in vitro* tests. AX requires protein haptentation to form multivalent conjugates with increased size to be immunogenic. Knowing adduct structural features for promoting effector cell activation would help to improve *in vitro* tests. We aimed to identify the optimal structural requirement in specific cellular degranulation to AX using well-precised nanoarchitectures of different lengths.

**Method:** We constructed eight Bidendron Antigens (BiAns) based on polyethylene glycol (PEG) linkers of different lengths (600–12,000 Da), end-coupled with poly-amidoamine dendrons that were terminally multi-functionalized with amoxicilloyl (AXO). *In vitro* IgE recognition was studied by competitive radioallergosorbent test (RAST) and antibody–nanoarchitecture complexes by transmission electron microscopy (TEM). Their allergenic activity was evaluated using bone marrow-derived mast cells (MCs) passively sensitized with mouse monoclonal IgE against AX and humanized RBL-2H3 cells sensitized with polyclonal antibodies from sera of AX-allergic patients.

**Results:** All BiAns were recognized by AX-sIgE. Dose-dependent activation responses were observed in both cellular assays, only with longer structures, containing spacers in the range of PEG 6000–12,000 Da. Consistently, greater proportion of immunocomplexes and number of antibodies per complex for longer BiAns were visualized by TEM.

**Conclusions:** BiAns are valuable platforms to study the mechanism of effector cell activation. These nanomolecular tools have demonstrated the importance of the adduct size to promote effector cell activation in AX allergy, which will impact for improving *in vitro* diagnostics.

**Abbreviations:** AX, amoxicillin; AXO, amoxicilloyl; AXO-Bu, amoxicilloyl-butylamine; BiAn, bidendron antigens; DNP, dinitrophenyl; HSA, human serum albumin; Hum, human; MCs, mast cells; MoAbs, monoclonal antibodies; MW, molecular weight; PAMAM, polyamidoamine; PEG, polyethylene glycol; PLL, poly-L-lysine; RAST, radio allergosorbent test; RBL, rat basophilic leukemia cell; SAR, structure–activity relationship; TEM, transmission electron microscopy.

Torres and Montañez contributed equally to this work.

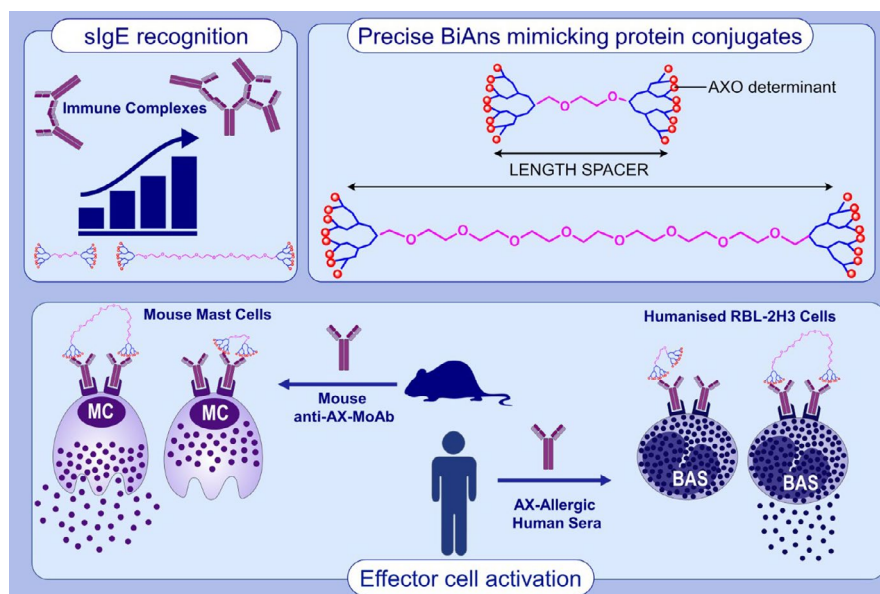
This is an open access article under the terms of the Creative Commons Attribution-NonCommercial-NoDerivs License, which permits use and distribution in any medium, provided the original work is properly cited, the use is non-commercial and no modifications or adaptations are made.

© 2021 EAACI and John Wiley and Sons A/S. Published by John Wiley and Sons Ltd.

PI17/01237, PI20/01734, PI20/01447,  
ARADYAL RD16/0006/0001 and  
Euronanomed Program AC19/00082

## KEYWORDS

amoxicillin, drug allergy, IgE cross-linking, immunocomplex, nanostructure



## GRAPHICAL ABSTRACT

The use of BiAns demonstrates the importance of adduct size and distance between determinants to promote effector cell activation in AX allergy. Optimal effector cell activation is shown with the biggest BiAns, which involves a greater number of immunocomplex and antibodies. BiAns are versatile nanoplateforms that can be applied to different allergies, valuable for improving *in vitro* allergy tests. Abbreviations: AX, amoxicillin; AXO, amoxicilloyl; BiAn, bidendron antigen; MoAb, monoclonal antibody; RBL, rat basophilic leukemia cell

## 1 | INTRODUCTION

Drug allergy accounts for 5–10% of all adverse drug reactions and could result in life-threatening complications.<sup>1,2</sup>  $\beta$ -lactam antibiotics are the most frequent triggers of reactions, with amoxicillin (AX) as the most common elicitor nowadays.<sup>3</sup>  $\beta$ -lactam allergy can be induced by different immune mechanisms, among which the IgE antibody-mediated one is the most common and better studied.<sup>4,5</sup> The diagnosis of immediate reactions to AX is based mainly on *in vivo* and *in vitro* methods,<sup>6</sup> being drug provocation test the gold standard, although it is risky and not recommended in patients with severe reactions.<sup>2,7,8</sup> *In vitro* tests are based on the determination of specific IgE (sIgE), with the commercial ImmunoCAP only detecting 20% of allergic patients, and on the quantification of basophil activation after stimulation with the culprit drug,<sup>9,10</sup> showing sensitivity around 50%. Among the factors affecting such low sensitivity could be the fact that correct antigenic determinant and/or conjugates are not incorporated to *in vitro* tests.<sup>6,11,12</sup>

According to the hapten hypothesis, AX is a low molecular weight (MW) compound that must form protein covalent conjugates with increased size and multivalence to be immunogenic.<sup>13</sup> Spontaneous conjugation of AX occurs due to the structural propensity of its  $\beta$ -lactam ring opening by the nucleophilic primary amines from proteins that results in the amoxicilloyl (AXO) antigenic determinant.<sup>14</sup> The immunological recognition of such multivalently presented

antigenic determinants on a conjugate by, at least, two adjacent IgE antibodies that are bound to their high-affinity receptor (Fc $\epsilon$ RI) on the surface of tissue mast cells (MCs) or circulating basophils, results in an intricate process of IgE cross-linking,<sup>15–18</sup> releasing preformed inflammatory mediators and eliciting the acute allergic response.<sup>15,19</sup> The efficiency of the stimulation on cell degranulation is dependent on many factors, including the drug antigenic determinant structure,<sup>18,20</sup> its valency on the conjugate or complete antigen,<sup>21,22</sup> the size of the conjugate,<sup>15,23</sup> the proximity of the IgE epitopes,<sup>24</sup> and the steric hindrance.<sup>16,24–26</sup>

The study of these complex cellular and structural restrictions in the *in vitro* activation of effector cells requires sophisticated structures that are well-defined and characterized to facilitate the interpretation of results. In this regard, different molecules have been designed to assess the influence of these parameters on the degranulation of MCs using synthetic haptens linked on bi- or multivalent structures. The most widely used experimental model utilizes the rat basophilic leukemia cell (RBL)/dinitrophenyl (DNP) and/or dansyl system, in which the RBL cells are primed with monoclonal IgE-DNP and/or IgE-dansyl antibodies, followed by stimulation with a multivalent haptenated structure to induce degranulation.<sup>15,16,18,23,26–30</sup> Dissimilar optimal sizes have been reported for effective cross-linking as a consequence of the diverse features of the synthetic allergen systems studied, differing in the density of haptens (or valency),<sup>23,30</sup> three-dimensional structure, flexibility<sup>23</sup>, or rigidity<sup>15,29,30</sup> of the structures.

However, owing to the complexity of real drug allergy scenario, this kind of structure–activity relationship (SAR) approach with nanostructures has never been addressed involving drugs (as haptens) or samples from allergic patients (drug-sIgE). Inspired by our previous design of dendrimeric antigens that permit controlling the size, multivalence (number of haptens), and three-dimensional structure,<sup>31,32</sup> and showed potential use for drug-sIgE quantification,<sup>33–37</sup> we propose a new related nanoarchitecture design to expand the interaction studies with the immune system.

Herein, we construct a set of symmetrical dendrimer-derived nanoarchitectures, called Bidendron Antigens (BiAns), in which two dendrons decorated with multiple units of AXO are separated by flexible polymeric spacers of different lengths (Figure 1), to evaluate the influence of the nanoarchitecture size for promoting the activation of effector cells that causes drug allergic reactions. This SAR study will help understand deeply the required distance between AXO determinants to activate basophils or MCs, which would be useful for improving the sensitivity of *in vitro* tests for diagnosing allergic reactions to AX.

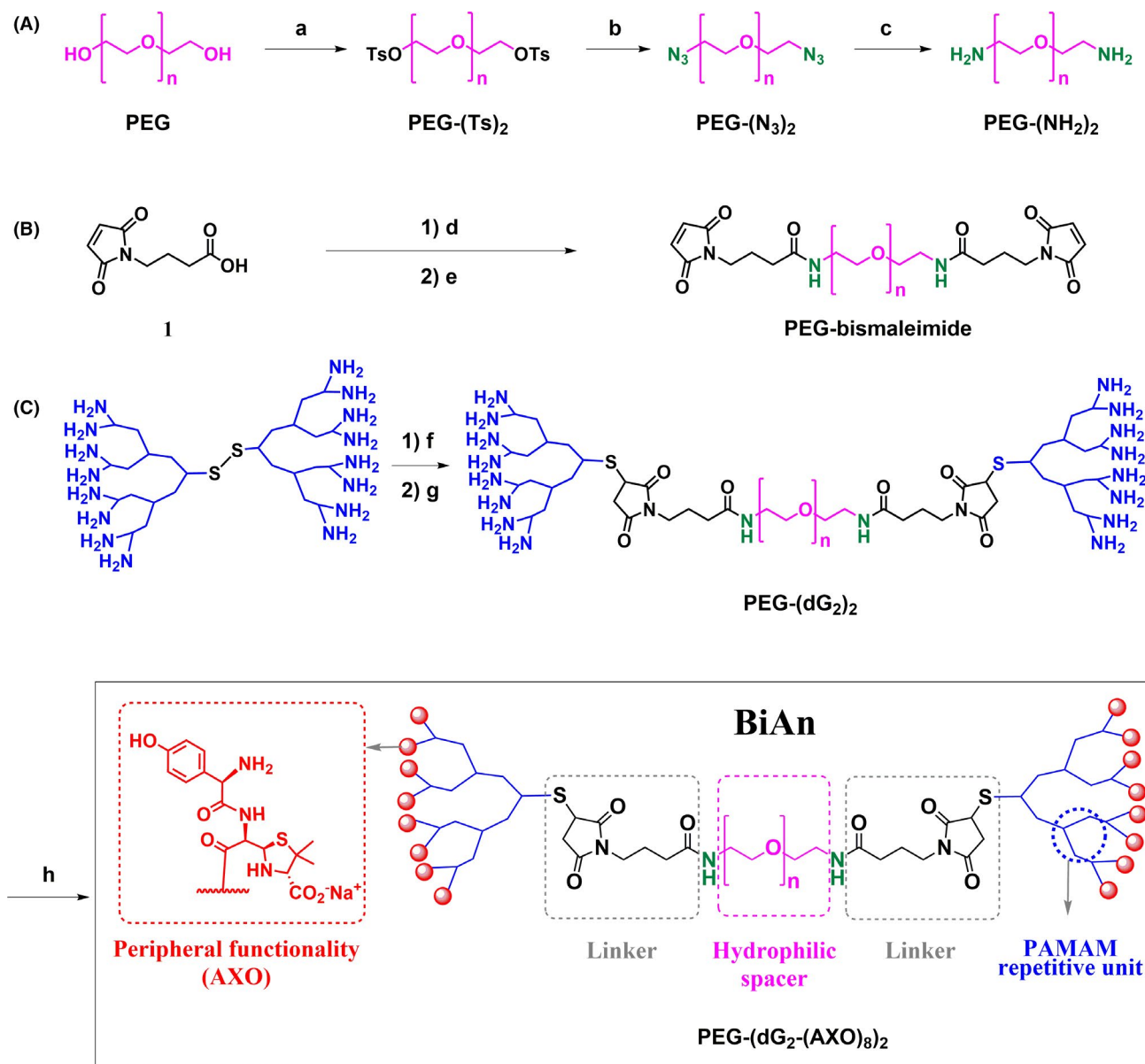


**FIGURE 1** General synthetic scheme including the following: (A) the intermediate PEG diamine; (B) the intermediate PEG-bismaleimide; and (C) the final BiAns, nanoarchitectures bearing 16 AXO determinants. The structural variation among different BiAns depends on the PEG length (with  $n$  ranging from 14 to 273). Briefly, the synthetic procedure consisted in obtaining bismaleimide-activated PEG compounds that allowed coupling between thiol-core dendrons (G2), whose peripheral groups were eventually functionalized with AX. In building up this, series of independent chemical reactions were followed, and the completion of the reactions was monitored by  $^1\text{H}$  and  $^{13}\text{C}$  NMR through the appearances and disappearances of distinctive signals. Reaction conditions: (a) TsCl,  $\text{CH}_2\text{Cl}_2$ , KOH,  $0^\circ\text{C}$ ; (b)  $\text{NaN}_3$ , THF- $\text{H}_2\text{O}$  (80:20), reflux at  $70^\circ\text{C}$ ; (c)  $\text{H}_2$ , Pd/C, MeOH, (d)  $^t\text{BuCOCl}$ , NMM,  $\text{CH}_2\text{Cl}_2$ ,  $0^\circ\text{C}$ ; (e) PEG-( $\text{NH}_2$ ) $_2$ ,  $\text{CH}_2\text{Cl}_2$ ; (f) PBS, pH 6.5, TCEP; (g) PEG-bismaleimide,  $\text{H}_2\text{O}$ , DMSO; (h) AX, carbonate buffer (0.05M, pH 10)

## 2 | METHODS

### 2.1 | Patients

Patients with a clinical history of immediate allergy to AX and tolerant subjects were evaluated following the European Academy of Allergy and Clinical Immunology (EAACI) guidelines.<sup>38,39</sup> The study was conducted according to the Declaration of Helsinki principles and was approved by the Provincial Ethics Committee of Malaga. All subjects included in the study were informed orally and signed the corresponding informed consent.

For evaluation of AX-sIgE recognition, we used a pool of 14 sera from patients with positive skin tests to AX and high levels (>7%) of AX-sIgE measured by direct radioallergosorbent test (RAST). Patients' data are displayed in Table S1.

Sera with high levels of total IgE, measured by ImmunoCAP ( $\geq 250$  kU/L) were selected for humanized RBL-2H3 (HumRBL-2H3) cell evaluation studies: three patients allergic to AX, with high levels (>7%) of AX-sIgE measured by RAST (data shown in Table S2), and three tolerant subjects, with no reactivity to  $\beta$ -lactams.

### 2.2 | Production of Conjugates and Anti-AXO monoclonal antibodies (MoAbs)

The synthesis, purification, and characterization of the conjugate of human serum albumin (HSA) with AX (HSA-AXO) and the series of BiAn and intermediates, and the production of two hybridomae:<sup>40</sup> AO3.2, IgG<sub>2a</sub> isotype, and AO6.2, IgE isotype are detailed in the Methods section of this article's Online Repository.

### 2.3 | Radioimmunoassays

Radioimmunoassays were performed by RAST as previously described<sup>14</sup> using the poly-L-lysine (PLL) cellulose solid-phase conjugated to AX (AXO-PLL cellulose disks) and <sup>125</sup>I-anti-IgE.<sup>41</sup> Results were considered positive if they were higher than 2.5% of label uptake, which was the mean  $\pm$  2 SD of the negative control group.

Competitive inhibition immunoassays were carried out with a pool of sera with high RAST values (>7%), which was incubated with the inhibitors (AXO-butylamine (AXO-Bu) and BiAns) at four concentrations (30, 15, 3, and 0.3 mM of AXO equivalents) as the fluid phase for 18h at room temperature. Then, AXO-PLL solid-phase disks were added, followed by the described RAST protocol. Results were calculated as the percentage of inhibition using the non-inhibited serum as a control.

### 2.4 | Transmission electron microscopy

The samples were prepared according to optimized negative staining (OpNS).<sup>42</sup> From the different tested MoAbs to BiAn ratios, a

molar ratio of 8:1 was found to be the optimal condition. This ratio was used to incubate MoAbs with BiAn(600), BiAn(6000), and BiAn(10000) to evaluate differences in the obtained complexes as a function of the employed nanoarchitecture.

### 2.5 | Cell viability and activation assays

Viability was assessed using 3-(4,5-dimethylthiazol-2-yl)-5-(3-carboxymethoxyphenyl)-2-(4-sulfophenyl)-2H-tetrazolium (MTS) assay. Bone marrow cells were collected from femurs of BALB/c mice (4–6 weeks of age) from Charles River Laboratories (Saint Germain sur l'Arbresle) and cultured in DMEM with glucose and L-glutamine, fetal bovine serum, penicillin/streptomycin, and sodium pyruvate (all from Gibco, Life Technologies), plus recombinant murine SCF, IL-3, IL-9, and TGF- $\beta$  (all cytokines and growth factors were from Peprotech, Rocky Hill, NJ) to differentiate into MCs as previously described.<sup>43</sup> MCs were cultured for a minimum of 4 weeks and up to 8 weeks before they were used for functional assays. For activation through cross-linking of the IgE receptor, MCs were initially sensitized for 4h with 1  $\mu$ g/mL of mouse anti-AX IgE MoAb. After washing, MCs were resuspended in Tyrode's buffer and activated with the BiAns at 10, 50, and 100  $\mu$ M (concentration of AXO units) for 1h. A conjugate of HSA with AX at 50  $\mu$ g/ml (0.7  $\mu$ M of HSA-AXO, corresponding to 9, 7  $\mu$ M of AXO) was used as a positive control. Control experiments were performed in unsensitized cells. Experiments were performed in triplicate. All protocols involving animals followed the European legislation (Directive 2010/63/EU) and were approved by Comunidad de Madrid (Ref PROEX 089/15).

HumRBL-2H3 cells were obtained from the Cell Culture Unit of the University of Granada (Granada, Spain) and cultured in RPMI containing 10% heat-inactivated FBS, 2mM L-Glutamine, 100 IU/ml penicillin, and 100  $\mu$ g/ml streptomycin, in a humidified 5% CO<sub>2</sub> atmosphere at 37°C. HumRBL-2H3 cells were seeded in 96-well plates at a density of  $2 \times 10^5$  cells/well. Confluent growing HumRBL-2H3 cells were then sensitized with serum (50% v/v) from AX-allergic patients ( $n = 3$ ) and tolerant subjects ( $n = 3$ ) for 48 h at 37°C. Unsensitized cells were used as controls. Subsequently, cells were stimulated with the series of BiAns at different concentrations of AXO units (1, 10, 20, 50, 100, 150, and 200  $\mu$ M) for 2 h. In parallel experiments, cells were stimulated with the corresponding PEG linkers (structures without dendron-AXO), as negative controls. The HSA-AXO conjugate (at 10  $\mu$ M concentration of AXO) was used as a positive control of degranulation induction.

### 2.6 | Quantification of $\beta$ -hexosaminidase Release

The cell degranulation response was quantified measuring the level of  $\beta$ -hexosaminidase released in culture supernatants.<sup>44</sup> The percentage of  $\beta$ -hexosaminidase release was calculated as a percentage of the total  $\beta$ -hexosaminidase content. For further details, see the Methods section of this article's Online Repository.

### 3 | RESULTS

#### 3.1 | Design of Dendrimer-based Nanoarchitectures

A novel set of symmetrical dendrimer-derived nanoarchitectures, BiAns, was designed, synthesized (Figure 1), purified, and characterized (Figure S1). The BiAns were constructed to display critical design features: (a) bearing multiple units of AX antigenic determinant on the periphery of the dendron scaffolds to support multivalent interaction with the target antibody; (b) a flexible hydrophilic PEG spacer that provides a specific length between dendrons, promotes aqueous solubility,<sup>45</sup> and reduces non-specific protein adsorption, immunogenicity, and antigenicity.<sup>23,46</sup> A series of PEG chains of eight different average MWs (range 600–12,000 Da) were chosen as linkers. Commercially available second-generation ( $G_2$ ) polyamidoamine (PAMAM) dendron was selected as a common multivalent scaffold as it displays peripheral amino groups that covalently bind to AX in an efficient manner, and previous studies showed that dendrimeric antigens based on PAMAM are recognized by penicillin-sIgE.<sup>32,33,35,36</sup> The resulting BiAns encompass the same number of peripheral functionality (16 AXO per BiAn), differing only in the length of the hydrophilic spacer separating the dendrons, ranging in aqueous solution from 3 to 20 nm, with a maximal possible extension from 4.8 to 95.5 nm (Table 1).

#### 3.2 | IgE Recognition of BiAns

The ability of AX-sIgE to recognize BiAn conjugates was evaluated by competitive RAST inhibition immunoassays using sera from AX-allergic patients. This assay consists in competitive serum IgE recognition between the solid phase (AXO-PLL conjugate attached to cellulose disks) and the different inhibitors, containing AXO at different concentrations, in the fluid phase, and results are represented as % inhibition IgE binding (Figure 2). A butylamine-AXO monomeric conjugate was also employed as a control inhibitor.<sup>14</sup>

Assays were performed at equimolar amounts of AXO for all the conjugates, with a maximum concentration not higher than 30 mM of AXO, due to solubility issues at higher concentrations of BiAns. At such maximum concentration, sera were inhibited by all BiAns. In general, inhibition dropped at 3 and 0.3 mM of AXO in inhibitors. The presented data support that all compounds are recognized by AX-sIgE in a concentration-dependent manner, with no differences on the degree of IgE recognition among the different BiAns, as they present the same number of AXO equivalents (Figure 2).

#### 3.3 | Antibody–nanoarchitecture Complexes

To visualize IgE binding to the BiAn nanoarchitectures and the shape of the resulting immunocomplex, OpNS TEM was performed.<sup>47,48</sup> Optimization of the staining and imaging conditions with MoAb alone, AO3.2 (specific to AXO structure), showed Y-shaped monomeric antibodies in different orientations (Figure 3A) and their corresponding two  $F_{ab}$  and one  $F_c$  domains (Figure 3B).

To study the influence of spacer length of the BiAns on the formation of immunocomplexes, various nanoarchitectures (BiAn(600), BiAn(6000), and BiAn(10000)) were incubated with the antibody prior to evaluation of the complexes by OpNS TEM. In all cases, the immunocomplex formation followed a similar pattern, with most of the observed particles corresponding to individual antibodies (60–83%). Since the attached nanoarchitectures were not detectable, it was not possible to distinguish monomeric complexes from non-complexed antibodies. Considering only structures with more than one antibody per particle, the most predominant configuration corresponded to dimeric complexes, which appeared to be the most energetically favored structure (Figure 3C, Table S3). Since the length of the PEG spacer in the BiAn increased (PEG 10,000 > 6000 > 600), the percentage of complexes with 2 or more than 2 antibodies also increased. This might be ascribed to a larger steric hindrance in the structures with shorter PEG spacer, where the two AXO dendrons are much

TABLE 1 Estimated and experimental values of synthetic BiAns

Synthetic antigen	Estimated MW (Da)	Linker PEG MW (Da)	$(C_2H_4O)_N$ where N is	Flory radius (nm)	Solution PEG length (nm)	Extended PEG length: Contour length(nm)	$D$ ( $m^2/s$ )	Valency
BiAn 600	10,471.9	600	14	1.68	3.36	4.8	$1.53 \times 10^{-10}$	16
BiAn 1000	10,871.9	1000	23	2.28	4.56	8.0	$1.32 \times 10^{-10}$	16
BiAn 2000	11,871.9	2000	45	3.46	6.92	15.9	$1.29 \times 10^{-10}$	16
BiAn 4000	13,871.9	4000	91	5.24	10.48	31.8	$1.24 \times 10^{-10}$	16
BiAn 6000	15,871.9	6000	136	6.68	13.36	47.7	$1.09 \times 10^{-10}$	16
BiAn 8000	17,871.9	8000	182	7.94	15.88	63.6	$9.64 \times 10^{-11}$	16
BiAn 10000	19,871.9	10,000	227	9.08	18.16	79.5	$9.57 \times 10^{-11}$	16
BiAn 12000	21,871.9	12,000	273	10.13	20.26	95.5	$9.50 \times 10^{-11}$	16

Note: The Flory radius (RF) is calculated with  $RF = a.N^{1/5}$  (where  $a$  is the length of a monomer unit, and  $N$  the number of repeating monomeric units). Solution PEG length is calculated as the diameter of the polymer in aqueous solution based on Flory radius. The contour length (full extended length) is calculated as a product of the polymeric length ( $N$ ) and length of the monomeric unit, 3.5 Å for PEG.<sup>54</sup>

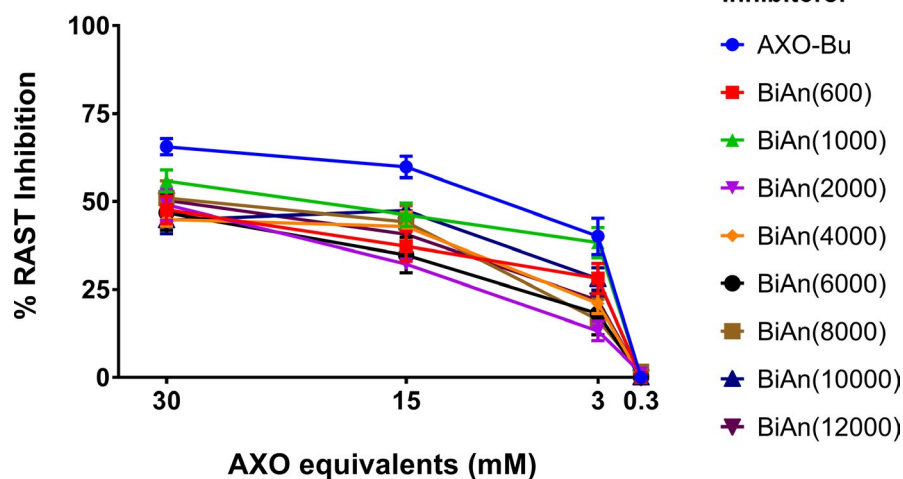


**FIGURE 2** RAST inhibition assays performed with a pool of sera from patients allergic to AX, using the series of BiAns and a AXO-Bu conjugate as inhibitors and cellulose disks modified with AXO-PLL as the solid phase. Specific IgE recognition is considered with inhibition of  $\geq 50\%$

closer to each other, preventing the binding of other antibodies to form the immunocomplex.

Besides the number of antibodies per complex, other differences could be also detected regarding the morphology of the complexes as a function of the studied molecule (Figure 3D). For complexes involving four antibodies with an open structure, up to three antibodies could be found to bind on a common spot (which could contain both dendrons of one BiAn). For larger complexes, conformational elucidation becomes extremely challenging due to the superposition of several antibodies. It is important to bear in mind that the antibody saturation conditions of the experiment may favor the formation of ring-closed complexes, and therefore minimize cross-linking potential. In this context, it is worth noting that all the complexes observed with **BiAn(600)** presented an open or linear structure (Figure 3D), which in the case of 2:2 complexes might correlate with the too-short spacer between both antigenic dendrons that impedes the simultaneous interaction with both recognition sites of a single antibody (Table 1), estimated in 11–13 nm.<sup>49</sup> On the other hand, and although open structures were still predominant, Figure 3D also shows some examples of ring-closed complexes with different numbers of antibodies per complex that were observed with **BiAn(6000)** (6.3% of the complexes) and **BiAn(10000)** (6.2%).

### 3.4 | Toxicity assay

Effect of different concentrations of BiAns on HumRBL-2H3 cell viability revealed a survival rate greater than 70% at most concentrations assayed. Only the highest one (200  $\mu\text{M}$ ) in **BiAn(2000)** and **BiAn(4000)** reduced the HumRBL-2H3 viability up to 64% (data not shown).

### 3.5 | Effects of BiAns on IgE activation of bone marrow-derived cells

The capacity of nanoarchitectures to induce IgE-dependent degranulation of bone marrow-derived MCs was evaluated. For this, cells

#### Inhibitors:

- AXO-Bu
- BiAn(600)
- ▲ BiAn(1000)
- ▼ BiAn(2000)
- ◆ BiAn(4000)
- BiAn(6000)
- BiAn(8000)
- ▲ BiAn(10000)
- ▼ BiAn(12000)

were sensitized with IgE MoAb against AX (specific to AX side chain), then treated with different concentrations of BiAns (in terms of the same equivalents of AXO), and afterward,  $\beta$ -hexosaminidase assay was performed (Figure 4, left). Stimulation of cells with HSA-AXO (10  $\mu\text{M}$  of AXO moieties) induced up to 25% of  $\beta$ -hexosaminidase release. However, cell stimulation with BiAns using an equivalent concentration of AXO only caused high activation with the **BiAn(10000)**, inducing 17% of  $\beta$ -hexosaminidase release. Only BiAns constructed with PEG of MW  $\geq 6000$  Da induced cell degranulation, and in a dose-dependent manner, showing up to 19% of  $\beta$ -hexosaminidase released at higher concentrations (50 and 100  $\mu\text{M}$  of AXO moieties), and bringing out the importance of the polymeric spacer length to achieve cell activation (Figure 4B). None of the BiAns tested induced cell degranulation on unsensitized cells (Figure 4A), indicating that activation occurs through an IgE mechanism.

### 3.6 | Effect of BiAns on IgE-induced degranulation in RBL-2H3 cells

Next, we chose the HumRBL-2H3 cell line for evaluation, which shares some characteristics with both MCs and basophils, and expresses human IgE receptor (Fc $\epsilon$ RI).<sup>27</sup> Cells were primed with polyclonal antibodies from sera of AX-allergic patients and tolerant subjects, then sensitized RBL-2H3 cells were treated with different concentrations of BiAns (in terms of the same equivalents of AXO determinants), and subsequently,  $\beta$ -hexosaminidase assay was performed. Results, shown in Figure 4 right, indicate that sensitized cells with sera from allergic patients and stimulated with BiAns containing PEG of MW  $\geq 6000$  Da significantly induced the  $\beta$ -hexosaminidase release in a concentration-dependent manner, compared with negative control groups (PBS and HSA activated cells) (Figure 4B bottom, Figure S3). Blank structure controls (PEGs) did not induce cell degranulation (Figure S3). Moreover, the highest concentrations of BiAns containing MW  $\geq 6000$  Da induced a release of 33% of  $\beta$ -hexosaminidase, similar to the one induced by HSA-AXO (at 10  $\mu\text{M}$  conc of AXO) (Figure 4B). Among these, **BiAn(10000)** and **BiAn(12000)** are the most effective intermolecular

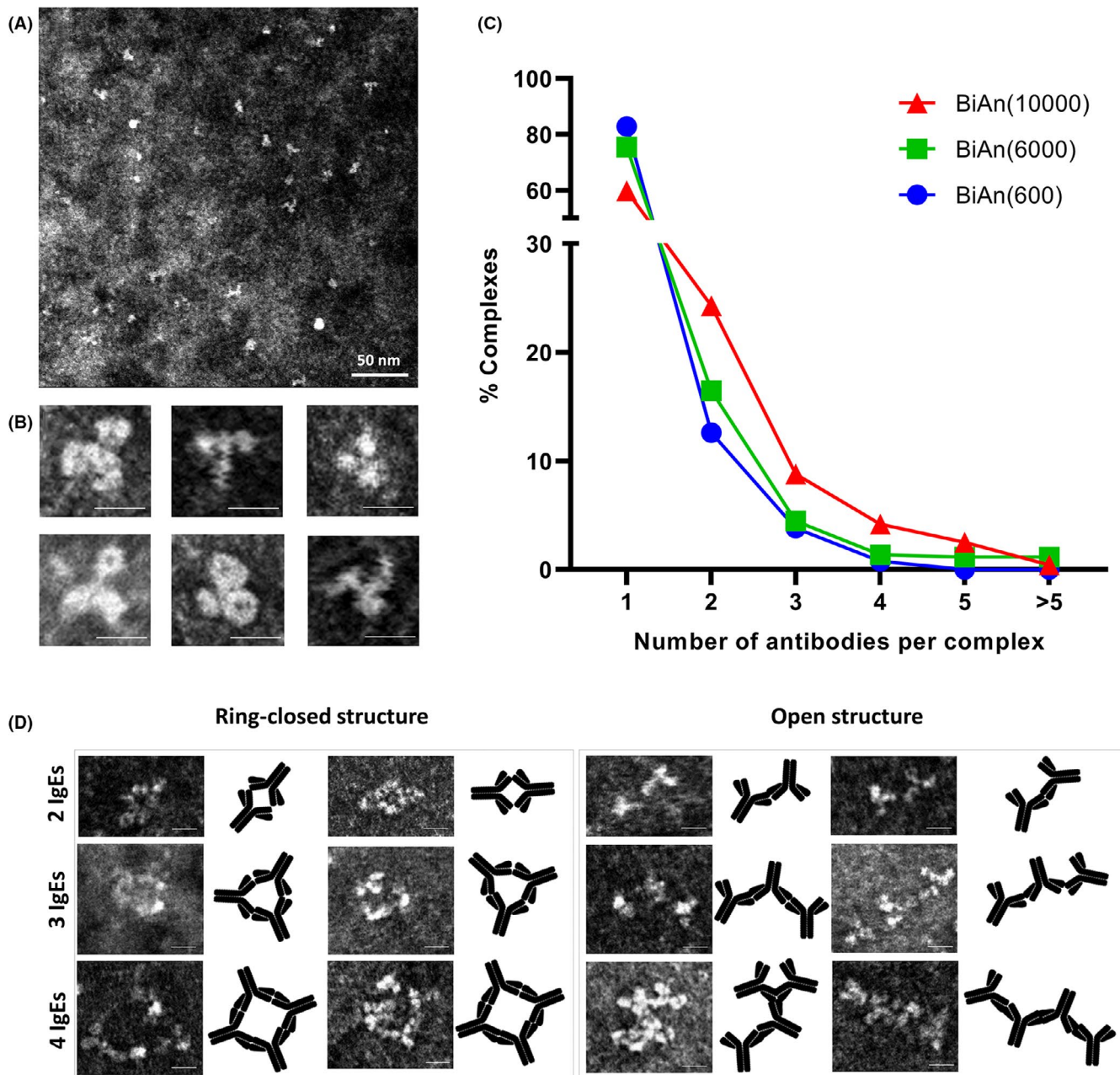


**FIGURE 3** Transmission electron micrograph of negatively stained MoAbs: (A) unbound MoAbs; (B) Zoomed-in views of selected individual antibody images. Scale bars represent 10 nm; (C) Number of MoAbs per complex after incubation with **BiAn(600)**, **BiAn(6000)**, or **BiAn(10000)**; (D) Zoomed-in views of selected individual complex images showing different open and ring-closed structures. Bars represent 10 nm

cross-linker as they induced above 27% of  $\beta$ -hexosaminidase release at 10, 50, and 100  $\mu$ M of AXO, although at lower concentration (1  $\mu$ M) only **BiAn(10000)** induced such substantial degranulation (Figure S3). No significant differences were observed in these BiAn treatments when the cells were sensitized with sera from tolerant subjects (Figure 4B top), and on unsensitized cells included as control of IgE activation (data not shown), whereas a more specific dose-response effect was observed when the cells were sensitized with sera from patients. The fact that none of the BiAn induced cell degranulation on unsensitized cells excludes direct activation by off-target occupancy of cell surface receptors. In addition, the absence of activation observed in parallel experiments with HMC 1.2 cell line, which exhibited

a similar phenotype to that of human MCs, expressing IgG receptor ( $Fc\gamma R$ ) but not the high-affinity IgE receptor ( $Fc\epsilon R$ ),<sup>50</sup> demonstrated that the BiAn do not trigger degranulation by an IgG-mediated pathway (Figure S4) suggesting that BiAn stimulate the degranulation on HumRBL-2H3 through an IgE pathway.

#### 4 | DISCUSSION

Our SAR study with well-characterized BiAn shows that the size and the proximity of AXO determinants on these conjugates influence the number and shape of immunocomplexes and their

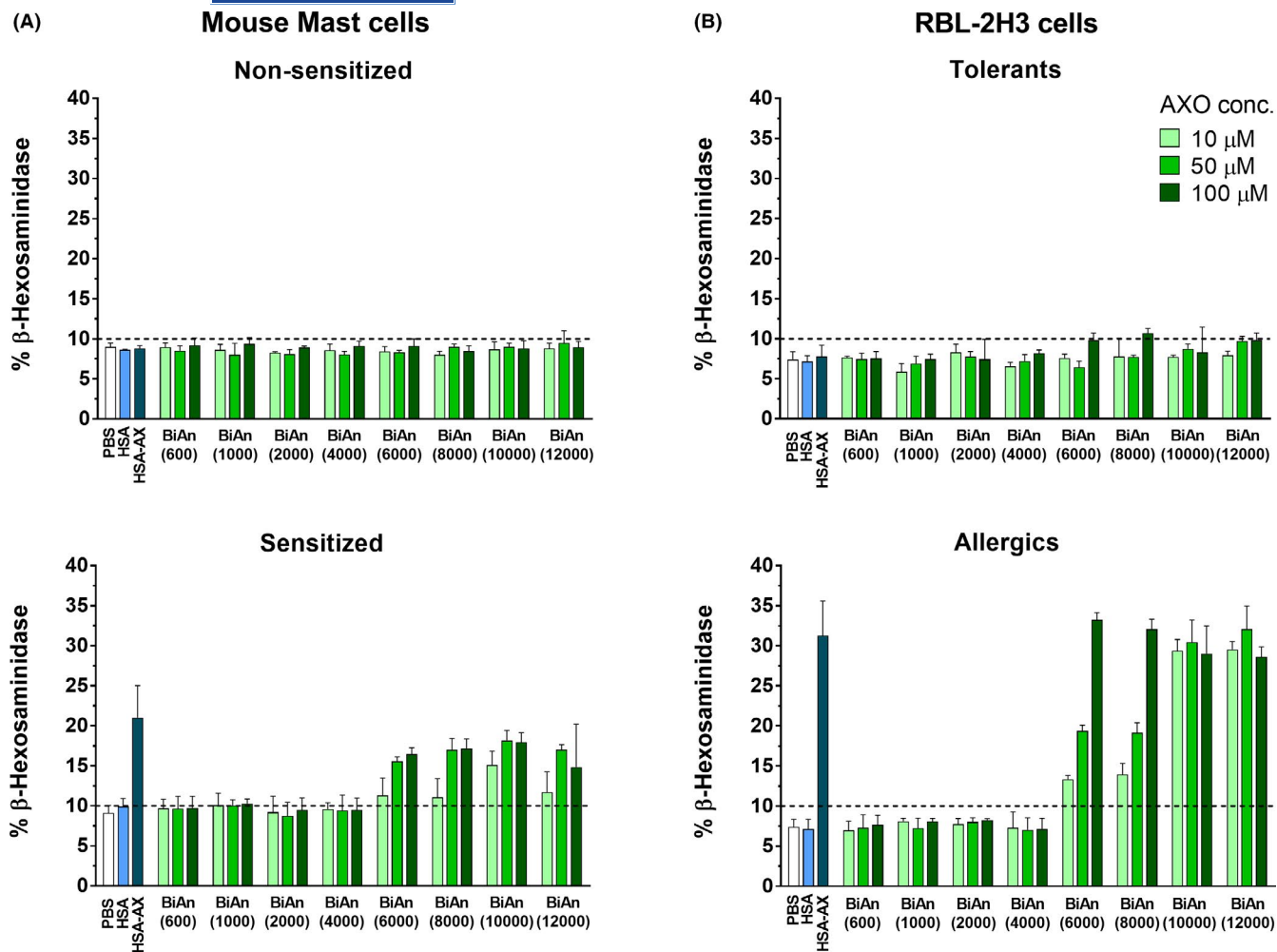


**FIGURE 4** Degranulation assays after incubation of cells with the series of BiAn at 10, 50, and 100  $\mu\text{M}$  of AXO equivalents. HSA and HSA-AXO (at 10  $\mu\text{M}$  of AXO) were used as negative and positive control, respectively. (A) Percentage of  $\beta$ -hexosaminidase release in unsensitized (top) and sensitized (bottom) bone marrow-derived MCs; (B) Percentage of  $\beta$ -hexosaminidase released by sensitized cells with sera from tolerant subjects (top) or with sera from AX-allergic patients (bottom). Data are expressed as means  $\pm$  SD. The baseline of percentage of  $\beta$ -hexosaminidase release is represented by the dotted horizontal line

subsequent ability to activate *in vitro* effector cells in an IgE-dependent mechanism. Through competitive immunoassays, it could be shown that all BiAn were recognized by AX-sIgE from patients. The higher concentration of determinants (AXO) increased the extent of inhibition, a pattern already reported with the monomeric AXO-Bu conjugate<sup>14</sup> and dendrimeric antigens with different penicillin determinants.<sup>32</sup> The increased inhibition obtained with the monomeric AXO-Bu, compared with BiAn, can be attributed to the absence of steric interactions for sIgE binding to AXO moieties in this small conjugate. In BiAn, PEG chains could contribute to a steric hindrance to the IgE binding, and also the high proximity of the eight AXO determinants exposed in each dendron would hinder their simultaneous IgE recognition. Using OpNS TEM, immunocomplexes could be visualized for different BiAn sizes. Assessment of BiAn immunogenicity at cellular level reveals that IgE-mediated degranulation of bone marrow-derived MCs and HumRBL-2H3 cells with BiAn is polymeric spacer length dependent. In both cellular assays, dose-dependent activation

responses were observed with all BiAn containing flexible linkers above a critical size (PEG 6000). Although these PEG polymers take on a spherical equilibrium configuration in an aqueous environment (for instance 13 nm for PEG 6000 in its folded conformation), their chain units move freely<sup>51</sup> and both ends could be at any position within the contour length of the polymer chain (~48 nm) (Table 1). Similar levels of activation were found between BiAn(10000) or BiAn(12000) compared with HSA-AXO activation at the same concentration of AXO in the RBL assays. However, in the case of MC, the same level of activation is only achieved with higher concentrations of BiAn. That could be explained by the better accessibility of AXO moieties on HSA-AXO which could allow the cross-linking of more than two IgE with a single molecule. On the other hand, given the proximity among the AXO units attached to the same dendron moiety, it is unlikely that more than two IgE are bound to each BiAn during cross-linking. OpNS TEM data support cellular activation results, since the BiAn that leads to a greater proportion of immunocomplexes, and the largest



number of antibodies per complex, was also the most successful one in activating cellular responses, in agreement with reported potent degranulation achieved by synthetic allergens with a valency  $\geq 3$ .<sup>29,30,52</sup>

The failure of BiAn containing PEG  $\leq 4000$  to stimulate degranulation indicates that, despite their recognition by AX-sIgE, they are inefficient at cross-linking cell surface IgE, which could be explained by a relatively low abundance of extended conformation of the PEG polymers in aqueous solution. BiAn containing the larger PEG length, and bearing equal valency, facilitates this interaction, presenting **BiAn(6000)** the minimal distance between haptens that can induce cell degranulation. The most potent stimulator **BiAn(10000)** is effective at all studied concentrations in both cell lines, MC and RBL-2H3 (as low as 1  $\mu\text{M}$  for RBL-2H3) (Figure S3), indicating that an estimated distance of  $\sim 18$  nm between haptens seems to be optimal for cross-linking the receptors. Consistent with the literature, this  $\sim 20$  nm dimension was found to be the optimal distance between DNP haptens on a rigid nanoparticle system to induce MC degranulation.<sup>30</sup> However, this is not in agreement with the pattern observed in DNP divalent and trivalent systems, in which rigid spacers of 4–5 nm stimulate stronger degranulation responses compared with those possessing spacing greater than 7–10 nm.<sup>15,29</sup> Our findings indicate that not only the size and multivalence of nanostructures are important factors for inducing degranulation, but also their flexibility.

Overall, these results suggest that BiAn nanoarchitectures containing longer PEG chains (MW range: 6000–12,000 Da) are effective triggers, whereas bivalent structures of DNP, in which haptens are also separated by flexible PEG of different lengths (MW range: 400–10,000 Da), were reported not to activate MC, but to behave as inhibitors.<sup>23</sup> This inhibition was explained by a preferential formation of intramolecular cross-linking of antibody by bivalent DNP of sufficient PEG length (10 nm) (stable 1:1 complexes),<sup>23</sup> or formation of cyclic dimers of IgE-Fc $\epsilon$ RI on the cell surface with shorter linkers ( $< 5$  nm).<sup>28</sup> Comparisons in terms of chemical structure between BiAn and DNP-PEG systems<sup>23</sup> points to multivalent vs. bivalent hapten presentation as the main difference. Likely, the multivalence of the dendron in BiAn favored IgE interaction, upon dendritic or synergistic effect, and therefore the degranulation. This is in agreement with cell activation induced by other multivalent systems: dendrimers presenting 16 units of DNP-induced MCs degranulation in DNP studies interaction;<sup>23</sup> different penicillin dendrimeric antigens activated basophils from patients, with increased stimulation index observed for those displaying higher valence (64 vs 16 haptens);<sup>53</sup> other rigid systems, nanoparticles ( $\geq 19.8$  nm) functionalized with multiple DNP, showed to be very effective effectors, however, a reduced hapten density inhibited degranulation.<sup>30</sup>

The scenario for MC and basophil degranulation is very complex, and the use of defined nanoarchitectures has allowed the identification of the minimal requirements for their activation in a realistic model. In this regard, multivalent dendritic presentation and distance between the haptens in BiAn constructed with PEG MW range 6000–12,000 fulfilled the optimal requirement to overcome the

intricate cellular preconditions leading to cell activation. The optimal distance between AXO determinants for effective cross-linking is observed in **BiAn(10000)**.

In summary, using multivalent AXO dendrons spaced by flexible PEG polymers, this study sheds light on the mechanism of the effector cells activation from a unique realistic perspective, using human samples and haptens in clinical use. Moreover, the synthesis of BiAn platform is versatile and could apply to different drug haptens or allergen epitopes. Understanding the biology and nanoscale organization of the cell membrane receptors can lead to the development of novel diagnostic and therapeutic tools for drug allergy.

## ACKNOWLEDGEMENTS

The characterization of nanostructures by mono and bidimensional NMR techniques as well as the optimization of TEM studies for visualising immunocomplex has been performed by the ICTS “NANBIOSIS”, more specifically by the U28 Unit of the Andalusian Centre for Nanomedicine & Biotechnology (BIONAND). The present study was supported by the Institute of Health “Carlos III” (ISCIII) of MINECO (grants cofunded by ERDF: “Una manera de hacer Europa” (grant numbers PI12/02529, PI15/01206, CP15/00103, PI17/01237, PI18/00095, PI20/01734, PI20/01447, RETICS ARADYAL RD16/0006/0001, Euronanomed Program AC19/00082); Andalusian Regional Ministry of Economy and Knowledge (grants cofunded by ERDF: “Andalucía se mueve con Europa”: grant no. CTS-06603); Andalusian Regional Ministry of Health (grant nos PI-0699-2011, PI-0179-2014); and “Premio UNICAJA a la innovación en biomedicina y salud.” AT has received funding from the European Union’s H2020 research and innovation program under the Marie Skłodowska-Curie (grant no. 713721). S.B. acknowledges financial support of Ministerio de Ciencia, Innovación y Universidades from Spain through a Juan de la Cierva Incorporación contract. C.M. holds “Nicolas Monardes” research contract by Andalusian Regional Ministry Health (grant no. RC-0004-2021). G.B. holds a “Juan Rodes” grant (JR18/00054), J.L.P holds a “Sara Borrell” grant (CD19/00250), A.R.N. and M.I.M. hold a “Miguel Servet I” grant (CP19/00191 and CP15/00103), both grants cofunded by European Social Fund (“El FSE invierte en futuro”). Tesfaye reports grants from Marie Skłodowska-Curie [grant No 713721], during the conduct of the study; in addition, Tesfaye has a patent PCT/ES2021/070103 pending. Dr. RODRIGUEZ NOGALES reports grants from ISCIII, during the conduct of the study; in addition, Dr. RODRIGUEZ NOGALES has a patent PCT/ES2021/070103 pending. Dr. Benede reports grants from Ministerio de Ciencia, Innovación y Universidades, during the conduct of the study. Dr. Fernandez reports grants from ISCIII, during the conduct of the study; In addition, Dr. Fernandez has a patent PCT/ES2021/070103 pending. Dr. Paris reports a Sara Borrell fellowship from ISCIII (CD19/00250), cofunded by European Social Fund. Dr. Rodriguez reports grants from ISCIII, during the conduct of the study. JIMÉNEZ-SÁNCHEZ reports grants from MICIN (PEJ2018-002865-A), during the conduct of the study; Dr. BOGAS HERRERA reports grants from ISCIII, during the conduct of the study. Dr. Mayorga reports grants

from ISCIII, from Andalusian Regional Ministry Health, during the conduct of the study; in addition, Dr. Mayorga has a patent PCT/ES2021/070103 pending. Dr. Torres reports grants from ISCIII, during the conduct of the study; in addition, Dr. Torres has a patent PCT/ES2021/070103 pending. Dr. Montañez reports grants from ISCIII, during the conduct of the study; in addition, Dr. Montañez has a patent PCT/ES2021/070103 pending. We thank Ms Claudia Corazza for her help with the English version of the manuscript.

### CONFLICT OF INTEREST

The authors declare that they have no known competing financial interests or personal relationships that could appear to influence the work reported in this paper.

### AUTHOR CONTRIBUTIONS

AT: Conceptualization, methodology, investigation, visualization, and writing—original draft. ARN: Methodology, investigation, and visualization. SB: Methodology, investigation, and visualization. TDF: Conceptualization, formal analysis, and writing—review and editing. JLP: Formal analysis and visualization. MJR: Investigation. IMJ: Investigation. GB: Investigation. CM: Conceptualization, supervision, and writing—review and editing. MJT: Conceptualization, resources, writing—review and editing, and funding acquisition. MIM: Conceptualization, methodology, visualization, writing—original draft, supervision, and funding acquisition.

### ORCID

Amene Tesfaye  <https://orcid.org/0000-0003-0482-8895>

Tahía D. Fernández  <https://orcid.org/0000-0003-0625-2156>

Cristobalina Mayorga  <https://orcid.org/0000-0001-8852-8077>

María J. Torres  <https://orcid.org/0000-0001-5228-471X>

María I. Montañez  <https://orcid.org/0000-0001-6641-5979>

### REFERENCES

- Warrington R, Silviu-Dan F, Wong T. Drug allergy. *Allergy Asthma Clin Immunol*. 2018;14(2):129–139.
- Demoly P, Adkinson NF, Brockow K, et al. International consensus on drug allergy. *Allergy* 2014;69(4):420–437.
- Doña I, Torres MJ, Montañez MI, Fernández TD. In vitro diagnostic testing for antibiotic allergy. *Allergy Asthma Immunol Res*. 2017;9(4):288.
- Salas M, Laguna JJ, Doña I, et al. Patients taking amoxicillin-clavulanic can become simultaneously sensitized to both drugs. *J Allergy Clin Immunol Pract*. 2017;5(3):694–702.e3.
- Solensky R, Khan DA, Contributors Leonard Bernstein WI, et al. Drug allergy: An updated practice parameter. *Ann Allergy, Asthma Immunol*. 2010;105(4):259–273.e78.
- Mayorga C, Celik G, Rouzair P, et al. In vitro tests for drug hypersensitivity reactions: an ENDA/EAACI Drug Allergy Interest Group position paper. *Allergy* 2016;71(8):1103–1134.
- Fernandez TD, Mayorga C, Salas M, et al. Evolution of diagnostic approaches in betalactam hypersensitivity. *Expert Rev Clin Pharmacol*. 2017;10(6):671–683.
- Torres MJ, Celik GE, Whitaker P, et al. A EAACI drug allergy interest group survey on how European allergy specialists deal with  $\beta$ -lactam allergy. *Allergy* 2019;74(6):1052–1062.
- Santos AF, Alpan O, Hoffmann H. Basophil activation test: mechanisms and considerations for use in clinical trials and clinical practice. *Allergy*. Published online 2021:0-2. <https://doi.org/10.1111/all.14747>
- Steiner M, Harrer A, Himly M. Basophil reactivity as biomarker in immediate drug hypersensitivity reactions—potential and limitations. *Front Pharmacol*. 2016;7, 171.
- Ariza A, Mayorga C, Bogas G, et al. Advances and novel developments in drug hypersensitivity diagnosis. *Allergy* 2020;75(12):3112–3123.
- Mayorga C, Fernandez TD, Montañez MI, Moreno E, Torres MJ. Recent developments and highlights in drug hypersensitivity. *Allergy* 2019;74(12):2368–2381.
- Pichler WJ, Beeler A, Keller M, et al. Pharmacological interaction of drugs with immune receptors: the p-i concept. *Allergol Int*. 2006;55(1):17–25.
- Ariza A, Mayorga C, Salas M, et al. The influence of the carrier molecule on amoxicillin recognition by specific IgE in patients with immediate hypersensitivity reactions to betalactams. *Sci Rep*. 2016;6(1):35113.
- Paar JM, Harris NT, Holowka D, Baird B. Bivalent ligands with rigid double-stranded DNA spacers reveal structural constraints on signaling by Fc $\epsilon$ RI. *J Immunol*. 2002;169(2):856–864.
- Handlogten MW, Kiziltepe T, Alves NJ, Bilgicer B. Synthetic allergen design reveals the significance of moderate affinity epitopes in mast cell degranulation. *ACS Chem Biol*. 2012;7(11):1796–1801.
- Deak PE, Kim B, Koh B, et al. Covalent heterobivalent inhibitor design for inhibition of IgE-dependent penicillin allergy in a murine model. *J Immunol*. 2019;203(1):21–30.
- Deak PE, Vrabel MR, Pizzutti VJ, Kiziltepe T, Bilgicer B. Nanoallergens: a multivalent platform for studying and evaluating potency of allergen epitopes in cellular degranulation. *Exp Biol Med*. 2016;241(9):996–1006.
- Deak PE, Kim B, Abdul Qayum A, et al. Designer covalent heterobivalent inhibitors prevent IgE-dependent responses to peanut allergen. *Proc Natl Acad Sci USA* 2019;116(18):8966–8974.
- Deak PE, Kim B, Adnan A, et al. Nanoallergen platform for detection of platin drug allergies. *J Allergy Clin Immunol*. 2019;143(5):1957–1960.e12.
- Puffer EB, Pontrello JK, Hollenbeck JJ, Kink JA, Kiessling LL. Activating B cells signalling with defined multivalent ligands. *ACS Chem Biol*. 2007;2(4):252–262.
- Xu K, Holowka D, Baird B, Goldstein B. Kinetics of multivalent antigen DNP-BSA binding to IgE-Fc $\epsilon$ RI in relationship to the stimulated tyrosine phosphorylation of Fc $\epsilon$ RI. *J Immunol*. 1998;160(7):3225–3235.
- Baird EJEJ, Holowka D, Coates GWGW, Baird B. Highly effective poly(ethylene glycol) architectures for specific inhibition of immune receptor activation. *Biochemistry* 2003;42(44):12739–12748.
- Gieras A, Linhart B, Roux KH, et al. IgE epitope proximity determines immune complex shape and effector cell activation capacity. *J Allergy Clin Immunol*. 2016;137(5):1557–1565.
- Hlavacek WS, Posner RG, Perelson AS. Steric effects on multivalent ligand-receptor binding: exclusion of ligand sites by bound cell surface receptors. *Biophys J*. 1999;76(6):3031–3043.
- Handlogten MW, Kiziltepe T, Serezani AP, Kaplan MH, Bilgicer B. Inhibition of weak-affinity epitope-IgE interactions prevents mast cell degranulation. *Nat Chem Biol*. 2013;9(12):789–795.
- Passante E, Frankish N. The RBL-2H3 cell line: Its provenance and suitability as a model for the mast cell. *Inflamm Res*. 2009;58(11):737–745.
- Posner RG, Subramanian K, Goldstein B, et al. Simultaneous cross-linking by two nontriggering bivalent ligands causes synergistic signaling of IgE Fc epsilon RI complexes. *J Immunol*. 1995;155(7):3601–3609.

29. Sil D, Lee JB, Luo D, Holowka D, Baird B. Trivalent ligands with rigid DNA spacers reveal structural requirements for IgE receptor signaling in RBL mast cells. *ACS Chem Biol*. 2007;2(10):674–684.
30. Huang YF, Liu H, Xiong X, Chen Y, Tan W. Nanoparticle-mediated IgE-receptor aggregation and signaling in RBL mast cells. *J Am Chem Soc*. 2009;131(47):17328–17334.
31. Montañez MI, Najera F, Perez-Inestrosa E. NMR Studies and molecular dynamic simulation of synthetic dendritic antigens. *Polymers (Basel)*. 2011;3(3):1533–1553.
32. Montañez MI, Najera F, Mayorga C, et al. Recognition of multiepitope dendrimeric antigens by human immunoglobulin E. *Nanomed Nanotechnol Biol Med*. 2015;11(3):579–588.
33. Montañez MI, Mayorga C, Torres MJ, Blanca M, Perez-Inestrosa E. Methodologies to anchor dendrimeric nanoconjugates to solid phase: toward an efficient in vitro detection of allergy to  $\beta$ -lactam antibiotics. *Nanomed Nanotechnol Biol Med*. 2011;7(6):682–685.
34. Montañez MI, Hed Y, Utsel S, et al. Bifunctional dendronized cellulose surfaces as biosensors. *Biomacromol* 2011;12(6):2114–2125.
35. Montañez MI, Perez-Inestrosa E, Suau R, Mayorga C, Torres MJ, Blanca M. Dendrimerized cellulose as a scaffold for artificial antigens with applications in drug allergy diagnosis. *Biomacromol* 2008;9(5):1461–1466.
36. Vida Y, Montañez MI, Collado D, et al. Dendrimeric antigen–silica particle composites: an innovative approach for IgE quantification. *J Mater Chem B*. 2013;1(24):3044.
37. Mayorga C, Perez-Inestrosa E, Rojo J, Ferrer M, Montañez M Role of nanostructures in allergy: diagnostics, treatments, and safety. *Allergy*. Published online February 9, 2021. Accepted Manuscript. <https://doi.org/10.1111/all.14764>
38. Romano A, Atanaskovic-Markovic M, Barbaud A, et al. Towards a more precise diagnosis of hypersensitivity to beta-lactams – an EAACI position paper. *Allergy* 2020;75(6):1300–1315.
39. Doña I, Romano A, Torres MJ. Algorithm for betalactam allergy diagnosis. *Allergy* 2019;74(9):1817–1819.
40. Mayorga C, Obispo T, Jimeno L, et al. Epitope mapping of  $\beta$ -lactam antibiotics with the use of monoclonal antibodies. *Toxicology* 1995;97(1–3):225–234.
41. Martín-Serrano A, Mayorga C, Barrionuevo E, et al. Design of an antigenic determinant of cefaclor: chemical structure–IgE recognition relationship. *J Allergy Clin Immunol*. 2020;145(4):1301–1304.e4.
42. Zhang L, Song J, Newhouse Y, Zhang S, Weisgraber KH, Ren G. An optimized negative-staining protocol of electron microscopy for apoE4•POPC lipoprotein. *J Lipid Res*. 2010;51(5):1228–1236.
43. Benedé S, Cody E, Agashe C, Berin MC. Immune characterization of bone marrow-derived models of mucosal and connective tissue mast cells. *Allergy Asthma Immunol Res*. 2018;10(3):268–277.
44. Benedé S, Ramos-Soriano J, Palomares F, et al. Peptide glycodendrimers as potential vaccines for olive pollen allergy. *Mol Pharm*. 2020;17(3):827–836.
45. Wang T, Zhang Y, Wei L, Teng YG, Honda T, Ojima I. Design, synthesis, and biological evaluations of asymmetric bow-tie PAMAM dendrimer-based conjugates for tumor-targeted drug delivery. *ACS Omega*. 2018;3(4):3717–3736.
46. Goswami LN, Houston ZH, Sarma SJ, Jalisatgi SS, Hawthorne MF. Organic & biomolecular chemistry efficient synthesis of diverse heterobifunctionalized clickable oligo(ethylene glycol) linkers: potential applications in bioconjugation and targeted drug delivery. *Org Biomol Chem*. 2013;11:1116.
47. Lin M, Krawitz D, Callahan MD, Deperalta G, Weckler AT. Characterization of ELISA antibody-antigen interaction using footprinting-mass spectrometry and negative staining transmission electron microscopy. *J Am Soc Mass Spectrom*. 2018;29:961–971.
48. Oda M, Uchiyama S, Noda M, et al. Effects of antibody affinity and antigen valence on molecular forms of immune complexes. *Mol Immunol*. 2009;47(2–3):357–364.
49. Schweitzer-Stenner R, Licht A, Liischer I, Pecht I. Oligomerization and ring closure of immunoglobulin E class antibodies by divalent haptens. *Biochemistry* 1987;26(12):3602–3612.
50. Jönsson F, Daéron M. Mast cells and company. *Front Immunol*. 2012;3:1–18.
51. Zhengyu M, David NLB, Sharon ML, et al. Tcr triggering by pMHC ligands tethered on surfaces via poly(ethylene glycol) depends on polymer length. *PLoS One* 2014;9(11):1–10.
52. Knol EF. Requirements for effective IgE cross-linking on mast cells and basophils. *Mol Nutr Food Res*. 2006;50(7):620–624.
53. Molina N, Martín-Serrano A, Fernandez T, et al. Dendrimeric antigens for drug allergy diagnosis: a new approach for basophil activation tests. *Molecules* 2018;23(5):1–13.
54. Zhang W, Martinelli J, Peters JA, et al. Surface PEG grafting density determines magnetic relaxation properties of Gd-loaded porous nanoparticles for MR imaging applications. *ACS Appl Mater Interfaces*. 2017;9(28):23458–23465. <https://doi.org/10.1021/acsami.7b05912>

## SUPPORTING INFORMATION

Additional supporting information may be found online in the Supporting Information section.

**How to cite this article:** Tesfaye A, Rodríguez-Nogales A, Benedé S, et al. Nanoarchitectures for efficient IgE cross-linking on effector cells to study amoxicillin allergy. *Allergy*. 2021;76:3183–3193. <https://doi.org/10.1111/all.14834>